

Supporting Information

Dual functional surface of MXene anode boosts long cyclability of lithium-metal batteries

Jeesoo Yoon, Oh B. Chae, Mihye Wu, Hee-Tae Jung**

J. Yoon, Prof. H.-T. Jung

National Laboratory for Organic Opto-electronic Materials, Department of Chemical and Biomolecular Engineering (BK21 four), Korea Advanced Institute of Science and Technology (KAIST), 291 Daehak-ro, Yuseong-gu, Daejeon, Korea

Center for KAIST-UC Berkeley-VNU Global Climate Change, Yuseong-gu, Daejeon 34141, Korea

heetae@kaist.ac.kr

Prof. M. Wu

School of International Engineering and Science, Jeonbuk National University, Jeonju-si, Jeonbuk State, 54896 Republic of Korea

Advanced Materials Division, Korea Research Institute of Chemical Technology, Yuseong-gu, Daejeon 34114, Korea

wumihye@jbnu.ac.kr

Prof. O.B. Chae

School of Chemical, Biological and Battery Engineering, Gachon University, Seongnam-si, Gyeonggi-do 13120, Republic of Korea

E-mail: obchae@gachon.ac.kr

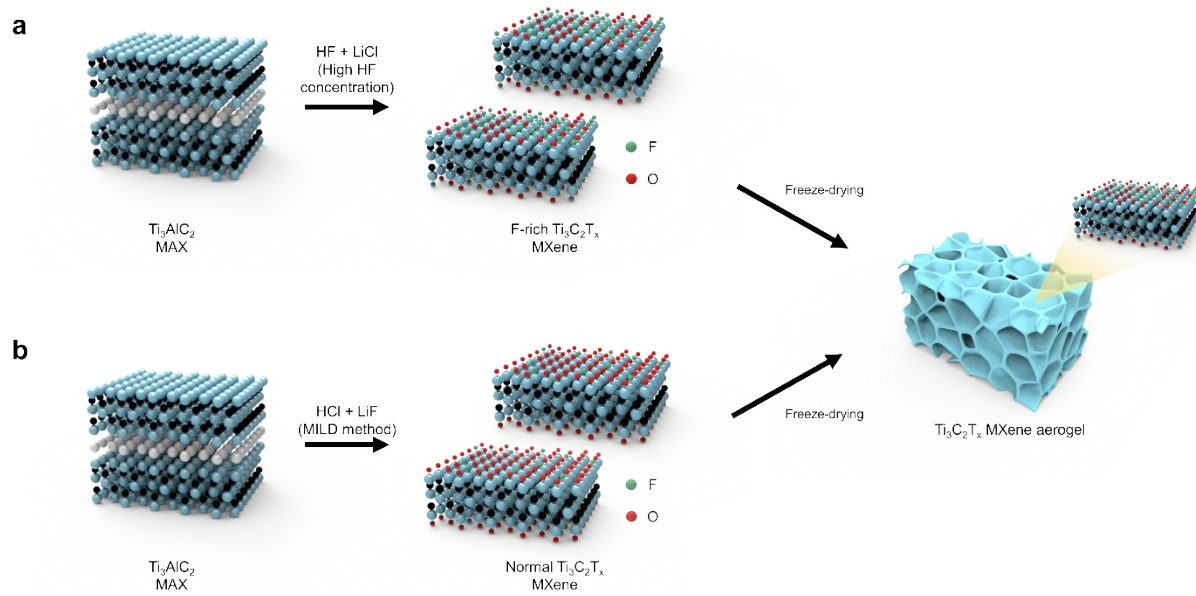


Figure S1. MXene termination control and 3 dimensional structure fabrication. a) F-rich $Ti_3C_2T_x$ MXene synthesis b) normal $Ti_3C_2T_x$ MXene synthesis.

$Ti_3C_2T_x$ MXene with different surface termination compositions was synthesized by the chemical wet-etching method utilizing different acid etchants. Both types of MXenes were freeze-dried into a freestanding 3 dimensional aerogel structure.

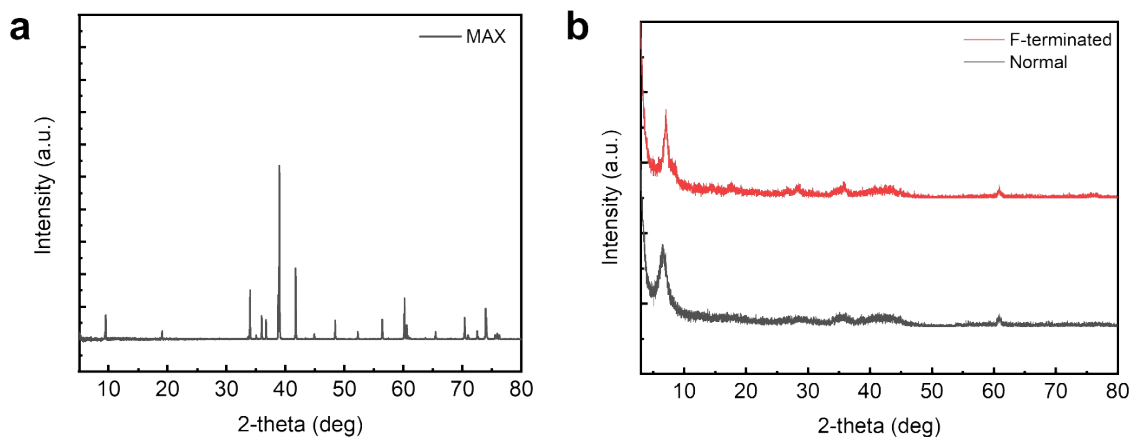


Figure S2. XRD analysis of a) Ti_3AlC_2 MAX phase, b) F-rich $\text{Ti}_3\text{C}_2\text{T}_x$, and c) normal $\text{Ti}_3\text{C}_2\text{T}_x$.

$\text{Ti}_3\text{C}_2\text{T}_x$ MXene was successfully synthesized by the chemical wet-etching method as verified through XRD. (002) peak of MAX phase at 9.5 degrees is shifted to lower angles after etching in both cases, confirming successful etching of Al layers in the MAX phase.

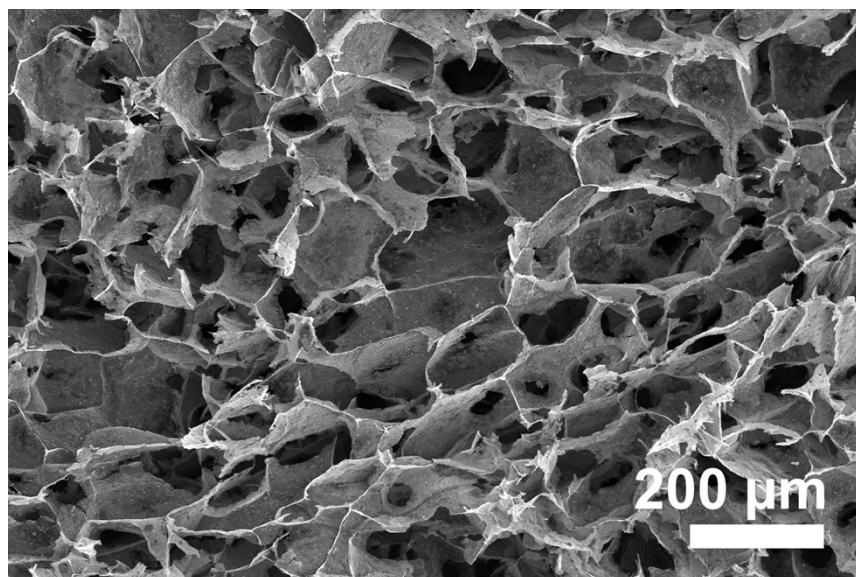


Figure S3. SEM image of Ti₃C₂T_x MXene aerogel.

Ti₃C₂T_x MXene was successfully fabricated into a highly porous aerogel structure by freeze-drying.

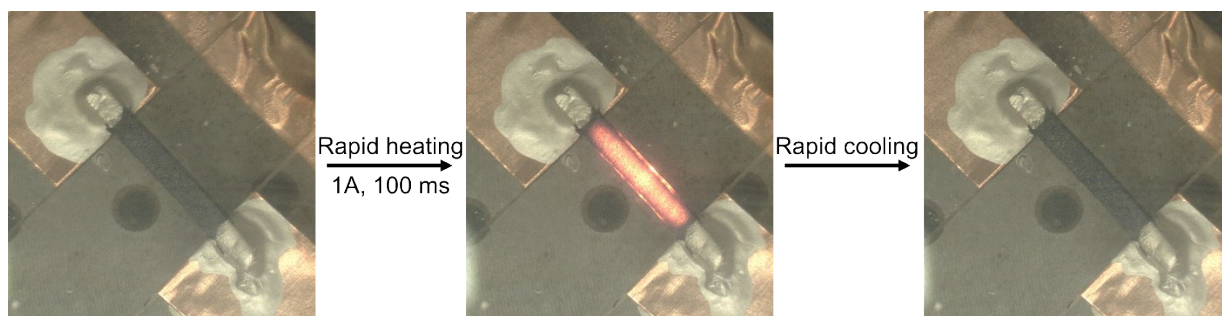


Figure S4. Rapid Joule heating of MXene aerogel.

An electric current of 1A was applied to the MXene aerogel for 100 milliseconds to induce rapid heating and cooling.

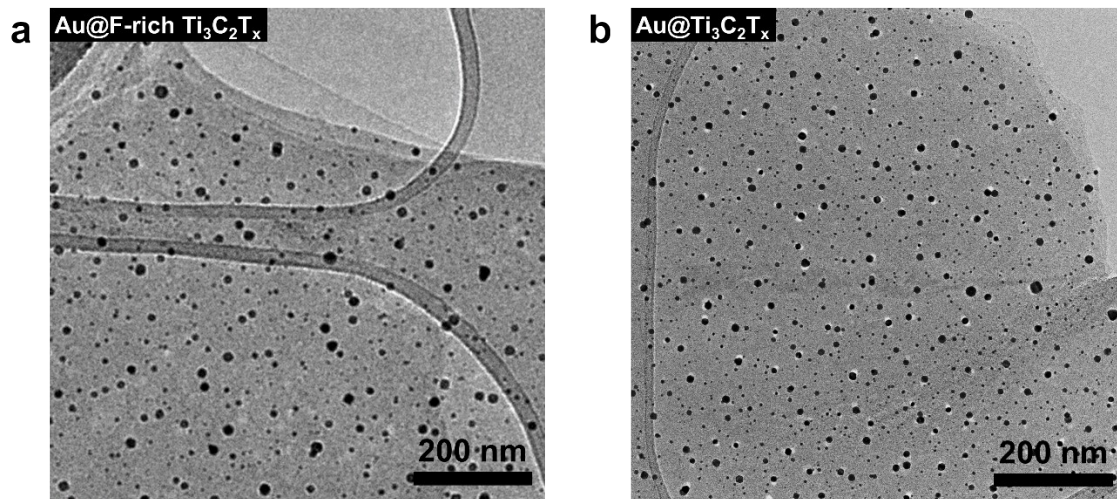


Figure S5. TEM image of a) Au@F-rich $Ti_3C_2T_x$ MXene and b) Au@ $Ti_3C_2T_x$ MXene.

Au NPs were homogeneously distributed over MXene surface regardless of the type of surface termination on its surface.

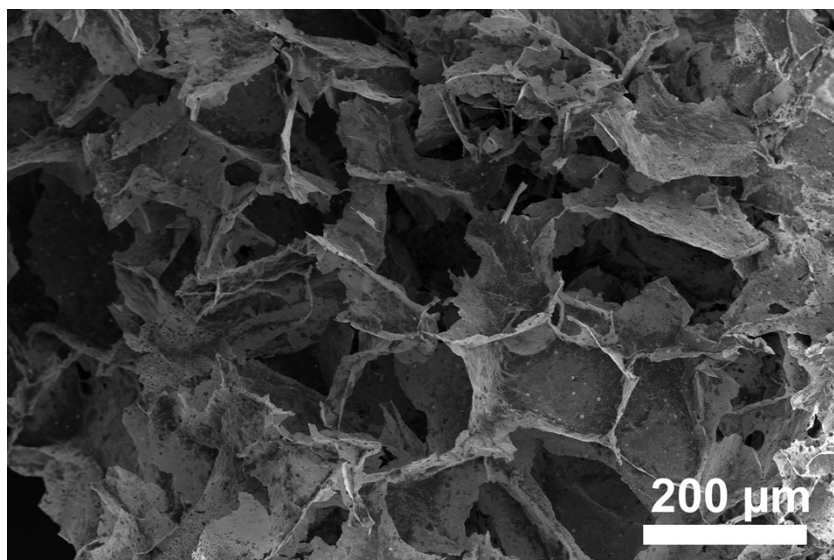


Figure S6. SEM image of Au@Ti₃C₂T_x MXene aerogel.

The Ti₃C₂T_x MXene aerogel retained its structure after rapid Joule heating, illustrating the non-destructive nature of the rapid Joule heating technique.

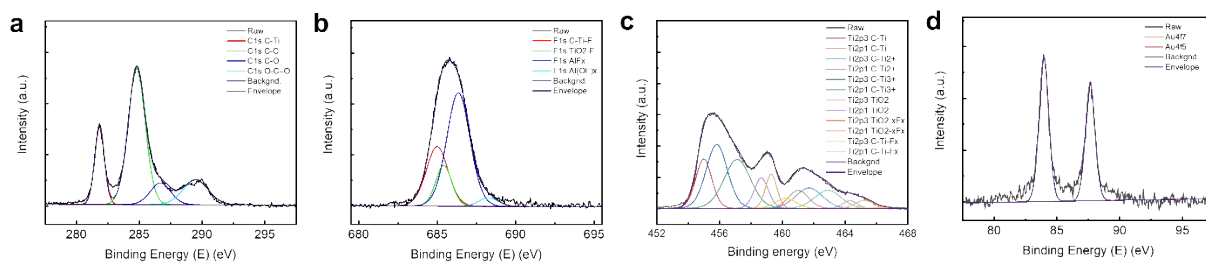


Figure S7. XPS peaks of Au@F-rich $Ti_3C_2T_x$ MXene. a) C1s peak. B) F1s peak. C) Ti2p peak. D) Au4f peak.

Au@F-rich $Ti_3C_2T_x$ MXene show clear formation of metallic gold NPs and a low degree of MXene oxidation. Even after rapid heating, the Au@F-rich $Ti_3C_2T_x$ MXene shows well-maintained abundant fluoride surface termination groups and minimum degradation of MXene.

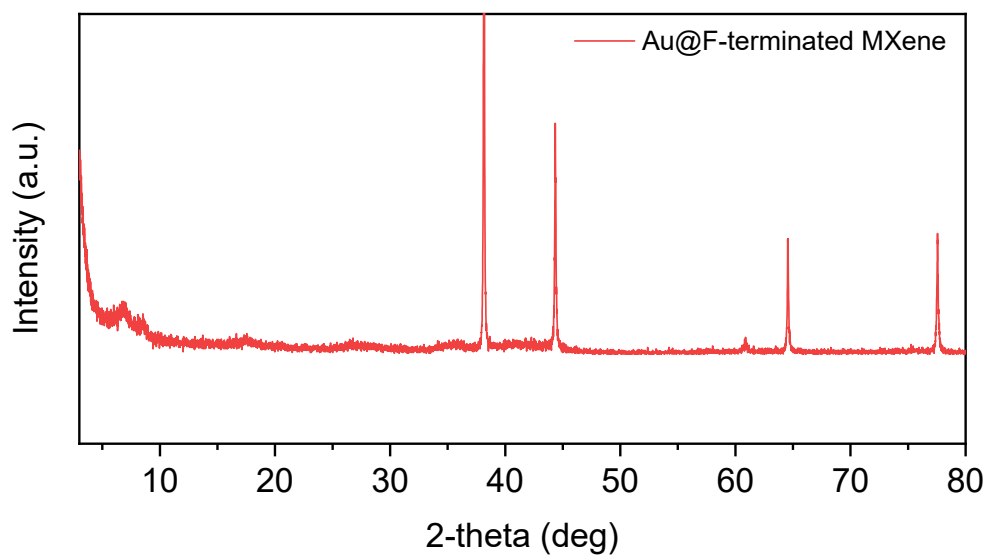


Figure S8. XRD peaks of Au@F-rich $\text{Ti}_3\text{C}_2\text{T}_x$ MXene.

The XRD peaks of Au@F-rich $\text{Ti}_3\text{C}_2\text{T}_x$ MXene show successful synthesis of Au NPs as illustrated by clear where peaks in 38.1, 44.2, 64.5 and 77.5 degrees.

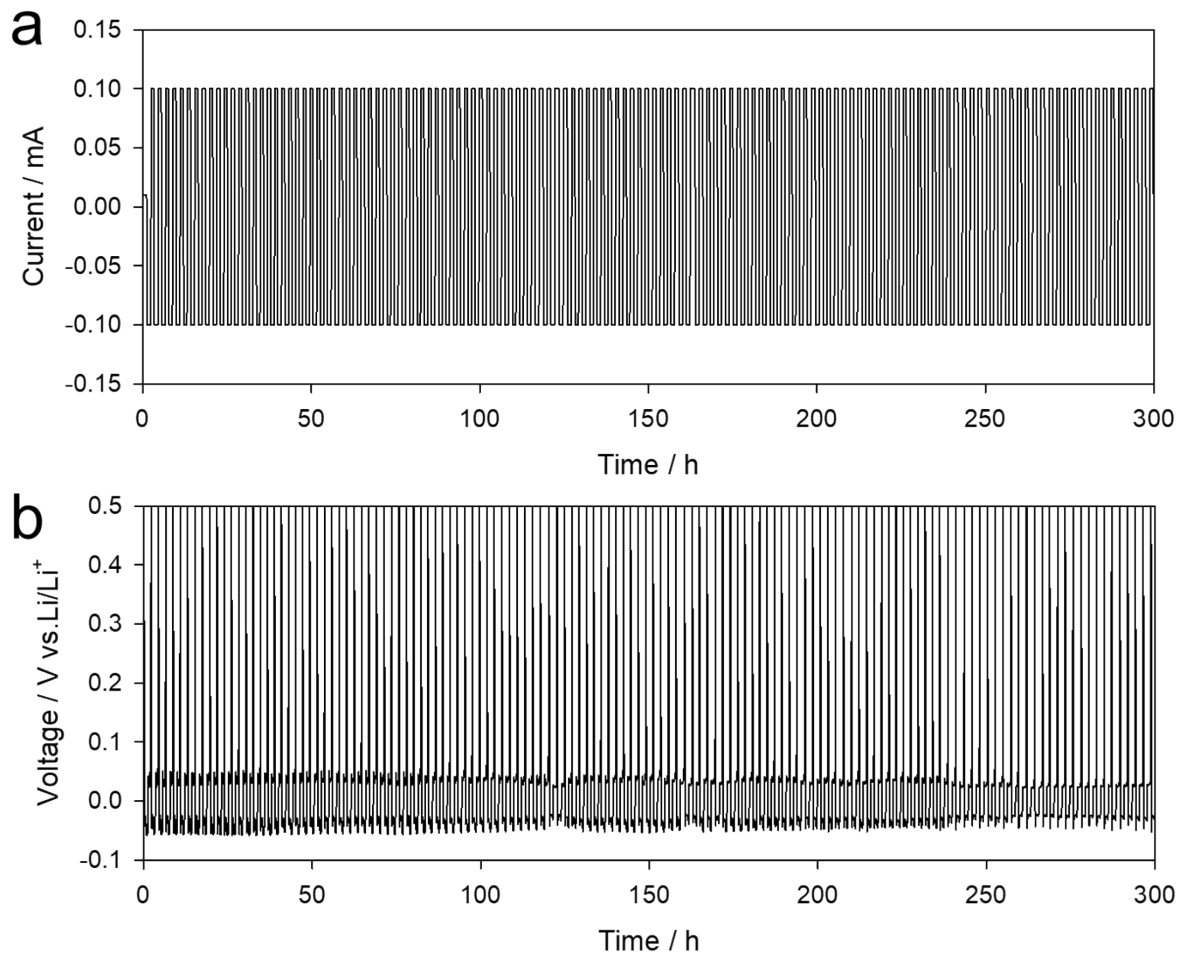


Figure S9. (a) Current-time (i-t) curve and (b) voltage-time (v-t) curve of Au@F-rich $\text{Ti}_3\text{C}_2\text{T}_x$ MXene.

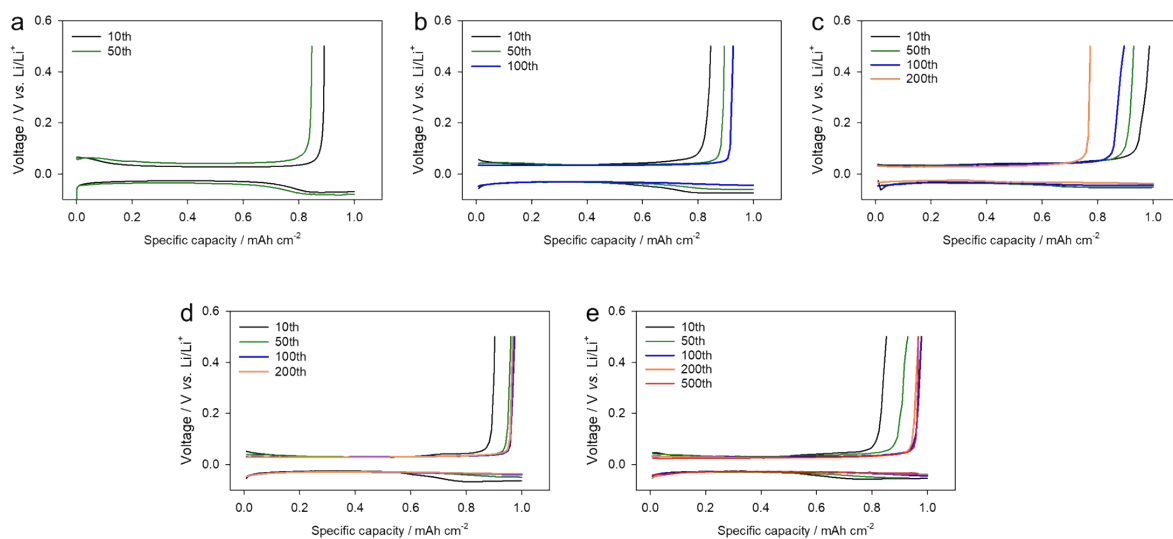


Figure S10. Voltage profiles of bare Cu foil and MXene at 1.0 mA cm^{-2} @ 1.0 mAh cm^{-2} , measured at selected cycles. (a) bare Cu foil (b) $\text{Ti}_3\text{C}_2\text{T}_x$ (c) $\text{Au@Ti}_3\text{C}_2\text{T}_x$ (d) F-rich $\text{Ti}_3\text{C}_2\text{T}_x$ and (e) $\text{Au@F-rich Ti}_3\text{C}_2\text{T}_x$.

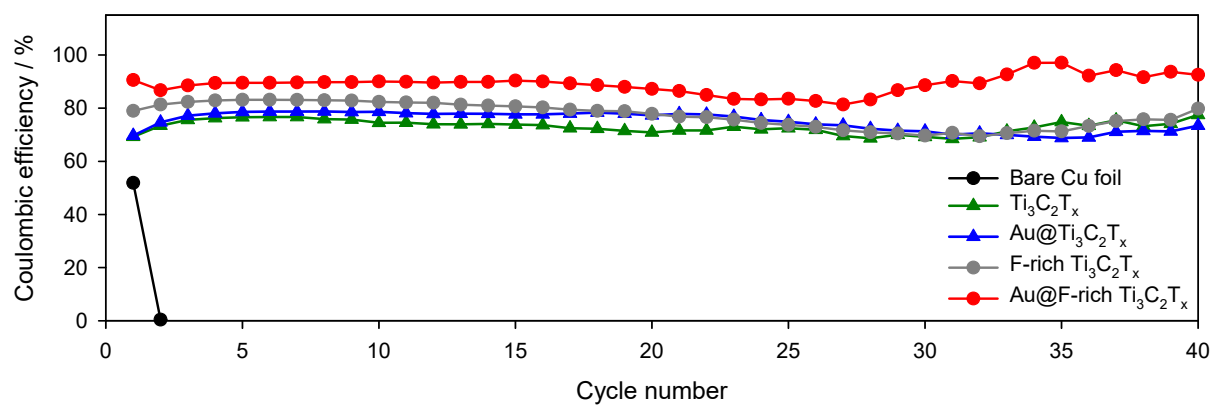


Figure S11. Cyclic performance of bare Cu foil and MXene at 5.0 mA cm^{-2} @ 3.0 mAh cm^{-2} .

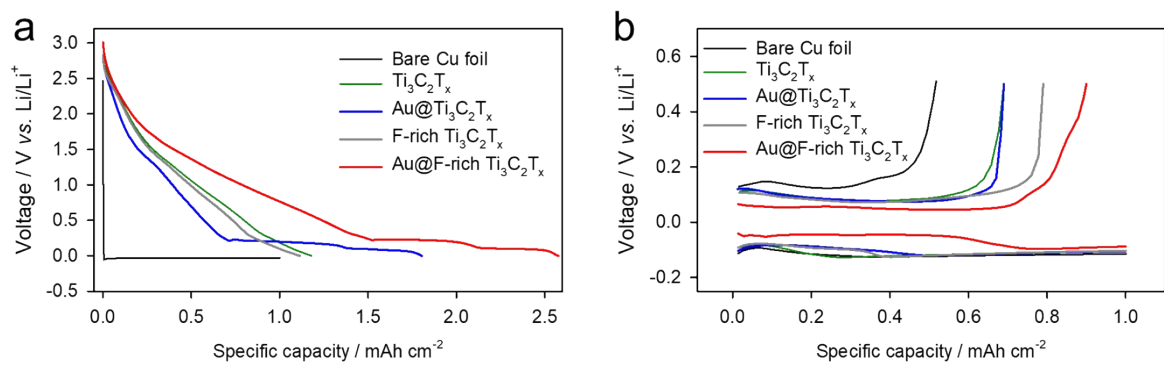


Figure S12. First voltage profiles of bare Cu and MXene at (a) 0.1 mA cm⁻² (b) 5.0 mA cm⁻²

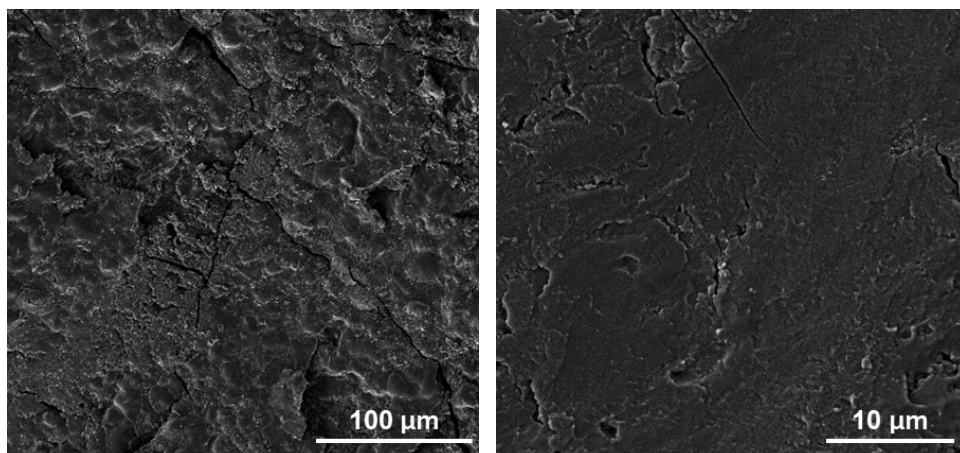


Figure S13. Ex situ SEM images of lithium deposition on Au@F-rich $\text{Ti}_3\text{C}_2\text{T}_x$ after cycling.

To assess the stability of Au@F-rich $\text{Ti}_3\text{C}_2\text{T}_x$, the cell was disassembled after 600 cycles, and the surface was examined using SEM imaging. The low-magnification SEM images revealed a uniform surface with lithium dendrite suppression.

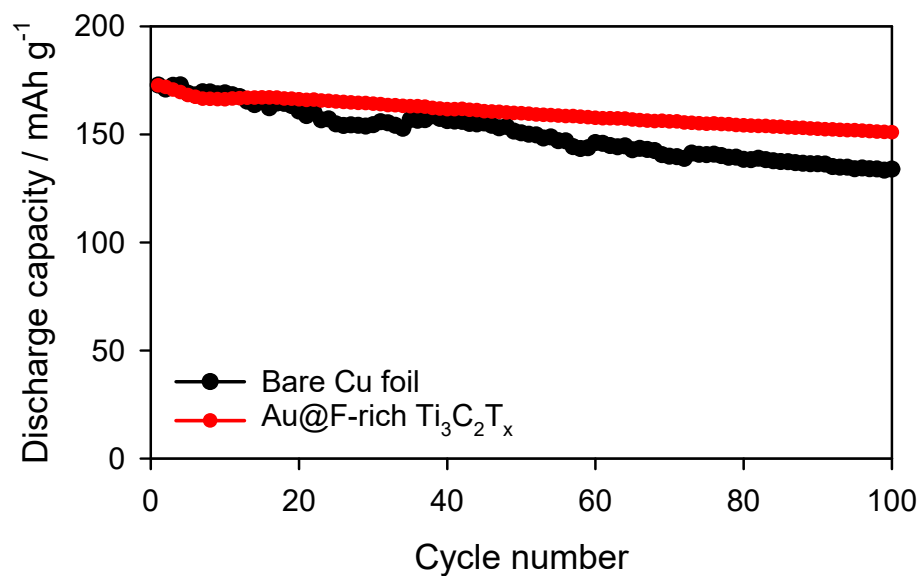


Figure S14. Cycle life of a $\text{LiNi}_{0.8}\text{Co}_{0.1}\text{Mn}_{0.1}\text{O}_2$ full cell assembled with the bare Cu foil and Au@F-rich $\text{Ti}_3\text{C}_2\text{T}_x$ at 0.5C.

Prior to constructing the full cell, the substrates were pre-deposited with lithium. The cells underwent a pre-cycling process at 0.1C, and subsequently, a 0.5C rate was applied to evaluate the cycle life.

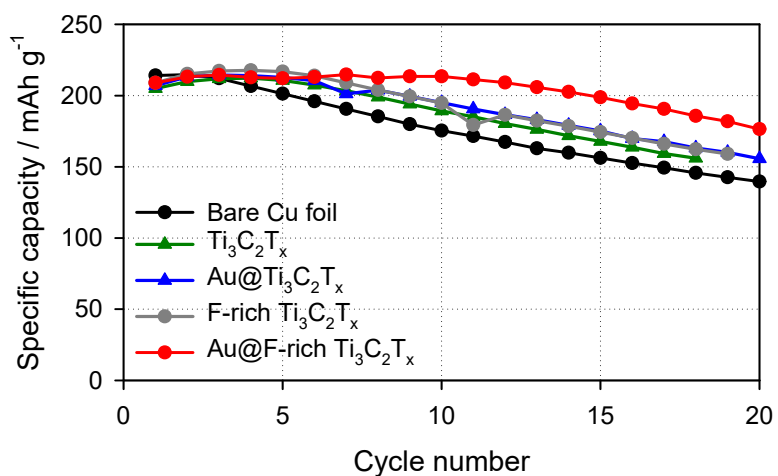


Figure S15. Cycle life of a $\text{LiNi}_{0.8}\text{Co}_{0.1}\text{Mn}_{0.1}\text{O}_2$ full cell assembled with the bare Cu foil and MXene without pre-deposition at 0.1C.

NCM811 full cells assembled with bare Cu foil and MXene without any pre-deposition of lithium. The cells were directly subjected to continuous cycling at 0.1C, and the cyclic stability was evaluated.